Journal of Alloys and Compounds, *188* (1992) 141–146
JALCOM 9037

Localization of cadmium in cadmium-containing hydroxy- and fluorapatites

A. Nounah and J. L. Lacout
Laboratoire des Matériaux, Physico-Chimie des Solides (URA CNRS 445), ENSCT–INPT, 38 rue des 36 ponts, 31400 Toulouse (France)
J. M. Savariault
Centre d'Elaboration de Matériaux et d'Etudes Structurales, CNRS, 29 rue Jeanne Marvig, 31055 Toulouse (France)

Abstract

Cadmium-containing hydroxyapatite and fluorapatite were prepared by a wet process in a basic medium and/or by a solid–gas reaction. Refinement of occupancy factor, using the Rietveld method, shows that the cadmium distribution is not strictly randomized between the two crystallographic cationic sites in the apatitic structure. Whatever the synthesis method used, cadmium has a slight preference for the Ca I site in fluorapatite and the Ca II site in hydroxyapatite.

1. Introduction

Calcium phosphates, especially synthetic or natural apatites, have been largely studied. They form the raw material of the phosphate fertilizer industry [1] and they are the main constituent of the mineral part of the hard living tissues: bones and teeth. They play an important role in the physiological and pathological behaviour of calcified tissues [2, 3].

Apatites form a large family of isomorphous compounds of phosphocalcium hydroxyapatite $Ca_{10}(PO_4)_6(OH)_2$. They generally crystallize in the hexagonal system (spatial group $P6_3/m$) [4]. The compact arrangement of PO_4 groups in the structure provides two kinds of channels containing calcium ions (Fig. 1). Ca I ions, four per unit cell, present a C_h site symmetry: they are surrounded by nine oxygen atoms (three O(1), three O(2) and three O(3)). Ca II ions, six per unit cell, present a C_s site symmetry and a coordination number of 7: they are surrounded by one O(1), one O(2), four O(3) and one another anion (an OH ion in the case of hydroxyapatite); this last anion occurs on the 6-fold axis near the intersection with the Ca II triangle; nevertheless its precise location depends on the type of ion it is.

Various substitutions occur in the apatitic structure, in both natural and synthetic compounds [5, 6, 7]; for instance, some sedimentary apatites contain cadmium. Cadmium is a toxic element which follows the alimentary chain from fertilizers to plants and finally accumulates in mammals [8, 9]. It can induce serious bone troubles, *e.g.* itaî-itaî illness, osteoporosis. Regulations for health protection tend to decrease the level of cadmium in fertilizers.

So, it is necessary to study the interactions of cadmium with calcium phosphate and especially the location of the cadmium in the apatitic structure for, firstly, eliminating this element from phosphate ores and fertilizers and, secondly, understanding the relation of cadmium with bone apatite. So, the studies of the calcium–cadmium substitution and of the location of cadmium in the apatitic structure present biological, geochemical and economic interests.

The substitution of Ca^{2+} with Cd^{2+} in hydroxyapatite is of extreme biological significance since it explains the mechanisms of incorporation of cadmium into the skeletal system.

Solid solutions of calcium and cadmium hydroxyapatite have been studied [10]. In the present paper, the distribution of cadmium between cationic sites I and II is proposed. The Rietveld method [11], modified by Young and Wiles [12, 13] is used for the determination of the occupancy number in each site.

2. Materials and method

The calcium–cadmium hydroxyapatites were precipitated using a double decomposition method in a boiling basic aqueous medium between a cationic solution containing $Ca(NO_3)_2{\cdot}4H_2O$–$Cd(NO_3)_2{\cdot}4H_2O$ and a phosphate solution containing $(NH_4)_2HPO_4$; fluorapatites were prepared either by a similar precipitation in the presence of a large excess of fluoride ions or by a

0925-8388/92/$5.00

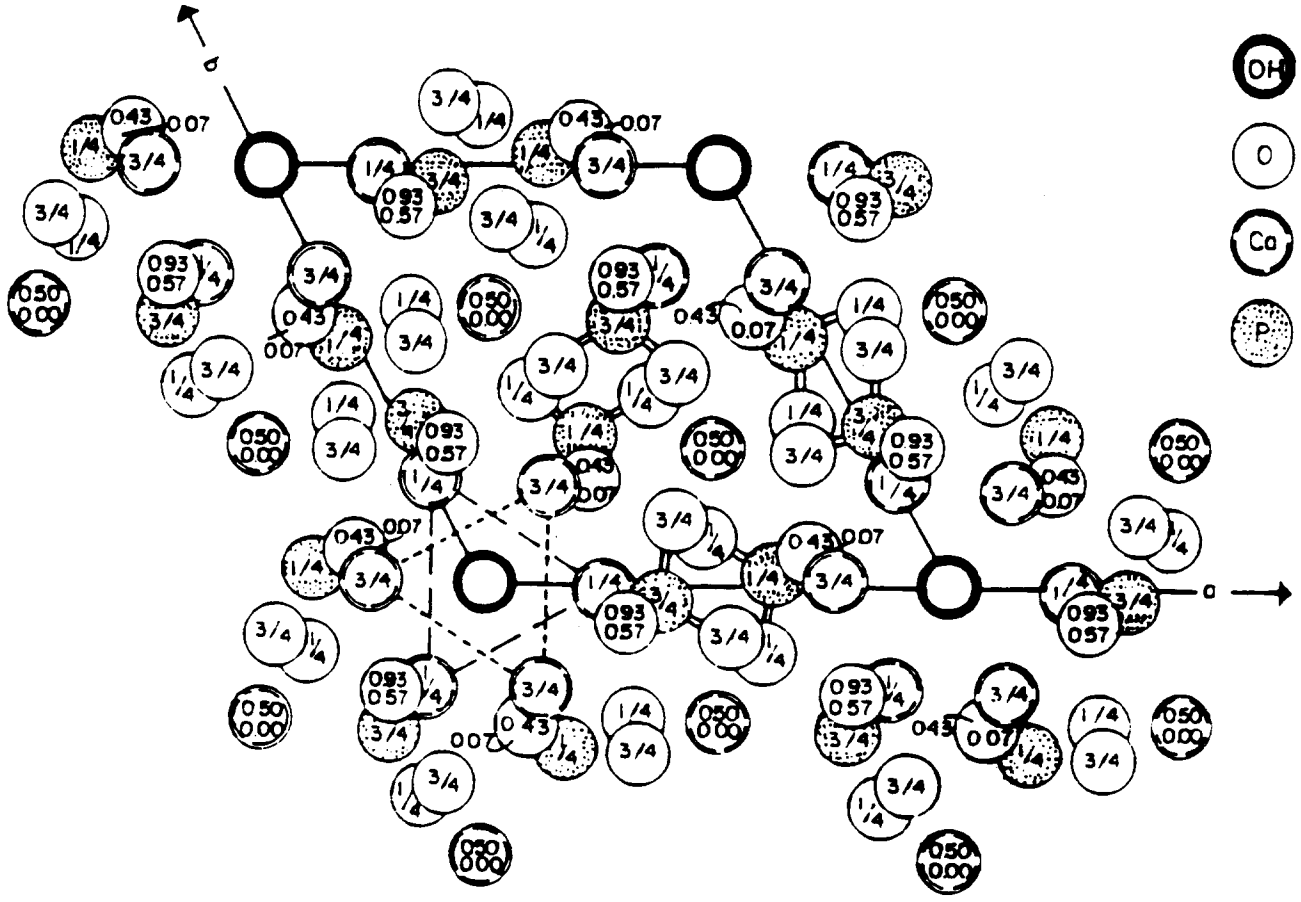

Fig. 1. Hydroxyapatite structure projected on $x-y$ plane [4].

solid–gas reaction at 600 °C between a previously prepared hydroxyapatite and hydrogen fluoride. All the samples were characterized by X-ray diffraction (CPS120 INEL instrument), IR spectrometry (FTIR PE7700 instrument) and chemical analysis.

A solid solution exists between calcium hydroxyapatite and cadmium hydroxyapatite; its formula is $Ca_{10-x}Cd_x(PO_4)_6(OH)_2$ with $0 \leqslant x \leqslant 10$; for the fluorapatite $Ca_{10-x}Cd_x(PO_4)_6F_2$, the solid solution only exists in the range $0 \leqslant x \leqslant 6$. When the Ca:(Ca + Cd) atomic ratio is greater than 6 (*i.e.* $x > 6$) the compounds obtained are mixed hydroxyfluoroapatites, and the amount of hydroxyl ions increases with the amount of cadmium ions; solid–gas compounds are a mixture of various phases.

All the apatitic samples were well-crystallized pure apatitic phases, with a cation:P atomic ratio near the stoichiometric value: 1.667. The a and c axis lattice constants of cadmium–calcium apatites vary linearly with composition according to Vegard's law; the slight shift to lower wavenumbers of the PO_4 and OH IR bands is due to the contraction of the unit cell and to the cation–oxygen interactions.

3. Structural analysis

Significant variations in line intensities were observed in the X-ray diffraction patterns of cadmium-containing apatites. These modifications were used to define the location of cadmium in the apatitic structure, using the well-known Rietveld refinement.

TABLE 1. Experimental conditions of X-ray diffractogram data collection

Radiation	Cu, $\lambda(K\alpha_1) = 1.5405$ Å, $\lambda(K\alpha_2) = 1.5443$ Å
Divergence slit	3.00 mm; Soller, 2.00 mm
Receiving slit	Soller, 0.10 mm
Beam width	10 mm
θ range	5°–80°
Step scan	$\theta-\theta$
Step width	0.01°
Count time per step	20 s from 5° to 40° and 40 s from 40° to 80°
Sample	Powder (particle size, <90 μm) is compressed on a sample holder of diameter 24 mm and depth 0.5 mm
Temperature	Room temperature

The Rietveld method allows a structure to be determined using intensities and profiles of X-ray lines, obtained from a powder pattern, when monocrystals are not available or when the properties are different to those of polycrystalline forms.

The Rietveld program was first described for neutron diffraction; Young and Wiles [12] adapted it for X-ray diffraction. A systematic study concluded that the best results were obtained with pseudo-Voigt (pV) and Pearson VII (PVII) profile functions [14]. The main parameters to be refined are the scale factor, the zero point of the diffraction pattern, the background, the unit cell dimensions, the atomic position parameters, the thermal factors and the profile parameters. The site occupancy factors were never simultaneously refined with the thermal parameters.

The program uses the Newton–Raphson algorithm to minimize the quantity

$$R = \sum wi[y_{i(\text{obs})} - y_{i(\text{cal})}]^2$$

by adjusting structural parameters and profile parameters. $y_{i(\text{obs})}$ and $y_{i(\text{cal})}$ are the observed and calculated

TABLE 2. Rietveld refinement

	HAP for the following values of N					FAP for the following values of N			HAF: $N = 2.0$
	0.0	0.5	1.0	2.0	4.0	0.5	1.0	3.0	
R_{wp}	15.2	13.2	12.4	11.5	10.2	12.5	12.1	10.5	11.0
R_p	11.0	9.9	9.4	8.8	7.0	9.7	9.4	8.1	8.3
R_B	6.2	6.5	6.3	6.4	5.2	6.7	6.6	5.6	6.0
R_F	6.0	4.7	4.8	5.1	4.5	5.0	4.8	4.3	5.2

N, number of cadmium atoms per unit cell; HAP, precipitated hydroxyapatite; FAP, precipitated fluorapatite; HAF, hydroxyapatite treated with NH_4F.

TABLE 3. Refined structural parameters

	x	y	z	N^a	B_{eq} (Å^2) [b]
$Ca_8Cd_2(PO_4)_6(OH)_2(Cd_{1.94})$ [c]					
O(1)	0.3266(8)	0.4846(8)	0.2500	6.00	0.8475
O(2)	0.5845(9)	0.4658(9)	0.2500	6.00	0.7360
O(3)	0.3418(6)	0.2562(6)	0.0688(7)	12.00	1.6463
P	0.3967(4)	0.3702(4)	0.2500	6.00	1.1001
Ca(1), Cd(1)	0.3333	0.6667	0.008(6)	0.54(1)	0.8369
Ca(2), Cd(2)	0.2472(2)	0.9931(3)	0.2500	1.40(2)	0.6988
OH	0.0000	0.0000	0.1921(19)	2.00	1.1595
$Ca_8Cd_2(PO_4)_6F_2(Cd_{2.04})$ [c, d]					
O(1)	0.3267(7)	0.4842(8)	0.2500	6.00	0.6274
O(2)	0.5871(9)	0.4677(9)	0.2500	6.00	1.0671
O(3)	0.3383(5)	0.2563(5)	0.0685(7)	12.00	1.0774
P	0.3969(4)	0.3688(4)	0.2500	6.00	0.7526
Ca(1), Cd(1)	0.3333	0.6667	0.0031(4)	0.96(1)	0.8547
Ca(2), Cd(2)	0.2444(2)	0.9928(3)	0.2500	1.08(2)	0.7617
F	0.0000	0.0000	0.2500	2.00	2.3093
$Ca_7Cd_3(PO_4)_6F_2(Cd_{3.05})$ [c]					
O(1)	0.3223(8)	0.4811(9)	0.2500	6.00	0.5132
O(2)	0.5845(10)	0.4665(10)	0.2500	6.00	0.6254
O(3)	0.3380(6)	0.2558(6)	0.0687(8)	12.00	1.9196
P	0.3986(5)	0.3720(5)	0.2500	6.00	0.9645
Ca(1), Cd(1)	0.3333	0.6667	0.0048(5)	1.36(2)	0.8875
Ca(2), Cd(2)	0.2438(3)	0.9920(3)	0.2500	1.69(3)	0.7627
F	0.0000	0.0000	0.2500	2.00	2.3473

[a]Atom numbers reported refer to cadmium atoms. The corresponding values for calcium atoms can be obtained from the difference of 4 for site I and of 6 for site II.

[b]Equivalent isotropic thermal parameters: $B_{eq} = 4(a^2\beta_{11} + b^2\beta_{22} + c^2\beta_{33} + ab\beta_{12}\cos\gamma)/3$

[c]Cadmium atoms per unit cell calculated from occupancy factors.

[d]Fluorapatite obtained by treatment of hydroxyapatite with NH_4F.

TABLE 4. Interatomic distances and bond angles

	$Ca_8Cd_2(PO_4)_6(OH)_2$	$Ca_8Cd_2(PO_4)_6F_2$ [a]	$Ca_7Cd_3(PO_4)_6F_2$
PO_4 tetrahedra			
Bond angles (deg)			
$O(1)^{i}$–P–$O(2)^{i}$	111.5(4)	110.6(4)	113.6(5)
$O(1)^{i}$–P–$O(3)^{i,iv}$ (×2)	112.2(3)	110.7(3)	110.1(3)
$O(2)^{i}$–P–$O(3)^{i,iv}$ (×2)	107.1(3)	108.7(3)	108.7(4)
$O(3)^{i}$–P–$O(3)^{iv}$	106.3(4)	107.3(3)	105.3(4)
Interatomic distances (Å)			
P–$O(1)^{i}$	1.514(10)	1.522(9)	1.511(9)
P–$O(2)^{i}$	1.528(8)	1.545(7)	1.507(9)
P–$O(3)^{i,iv}$ (×2)	1.548(5)	1.540(5)	1.553(5)
O(1)–$O(3)^{i,iv}$ (×2)	2.542(9)	2.519(9)	2.512(10)
O(2)–$O(1)^{i}$	2.515(12)	2.522(12)	2.526(13)
O(2)–$O(3)^{i,iv}$ (×2)	2.475(6)	2.507(6)	2.487(7)
O(3)–$O(3)^{iv}$	2.478(9)	2.481(9)	2.470(9)
Environment of metal atoms			
M(1)–$O(1)^{i,ii,iii}$ (×3)	2.393(6)	2.381(6)	2.374(6)
M(1)–$O(2)^{iv,v,vi}$ (×3)	2.459(7)	2.465(7)	2.473(8)
M(1)–$O(3)^{i,ii,iii}$ (×3)	2.804(5)	2.831(5)	2.829(5)
M(2)–$O(1)^{iii}$	2.685(6)	2.682(6)	2.636(6)
M(2)–$O(2)^{ii}$	2.340(7)	2.342(7)	2.356(8)
M(2)–$O(3)^{i,vi}$ (×2)	2.497(5)	2.499(5)	2.495(5)
M(2)–$O(3)^{ii,iv}$ (×2)	2.316(5)	2.307(5)	2.299(5)
M(2)–$(OH, F)^{i}$	2.389(3)	2.326(2)	2.320(3)
M(2)–$M(2)^{i,v,vi}$ (×3)	4.081(4)	4.029(4)	4.019(5)

Symmetry codes: i, x, y, z; ii, $-y, x-y, z$; iii, $y-x, -x, z$; iv, $-x, -y, z+1/2$; v, $x-y, x, z+1/2$; vi, $y, y-x, z+1/2$.
[a]Fluorapatite obtained by treatment of hydroxyapatite with NH_4F.

intensities respectively for every point in the profile under the Bragg reflections and w_i is the statistical weight given to the data point.

The Bragg reflections in the pattern have a half-width that varies with the diffraction angle:

$$H_K = (U \tan^2\theta_K + V \tan\theta_K + W)^{1/2}$$

U, V and W are refinable parameters.

Powder X-ray diffraction was carried out with a Seifert XRD3000TT diffractometer controlled by an IBM PC microcomputer. The diffractometer was equipped with collimation and Soller slits, diffracted beam graphite monochromator and proportional detector. The experimental details for data collection are reported in Table 1.

The quantitative criteria of fit are the R factors. The program calculates four R factors:

$$R_{\omega p} = 100\left\{\sum W_i[y_{i(\text{obs})} - y_{i(\text{cal})}]^2 \Big/ \sum \omega_i[y_{i(\text{obs})}]^2\right\}^{1/2}$$

for the weighted pattern,

$$R_p = 100 \sum |y_{i(\text{obs})} - y_{i(\text{cal})}| \Big/ \sum |y_{i(\text{obs})}|$$

for the pattern,

$$R_B = 100 \sum |I_{(\text{"obs"})} - I_{(\text{cal})}| \Big/ \sum I_{(\text{"obs"})}$$

for the Bragg intensities and

$$R_F = 100 \sum |F_{(\text{"obs"})} - F_{(\text{cal})}| \Big/ \sum |F_{(\text{"obs"})}|$$

for the Structure amplitudes.

These calculated factors for samples containing cadmium in different percentages are given in Table 2. They show that the fit is quite good. In Table 3 the refined fractional coordinates, occupation factors and thermal factors for three structures are reported. Table 4 gives the corresponding interatomic distances and bond angles. Figure 2 shows the observed powder diffraction patterns and the difference between observed and calculated patterns.

4. Discussion

Generally the location in the apatitic structure is largely dependent on ion radius: site Ca I is smaller than Ca II and one would expect that ions larger than calcium would be located at the Ca II site. Nevertheless, some exceptions exist.

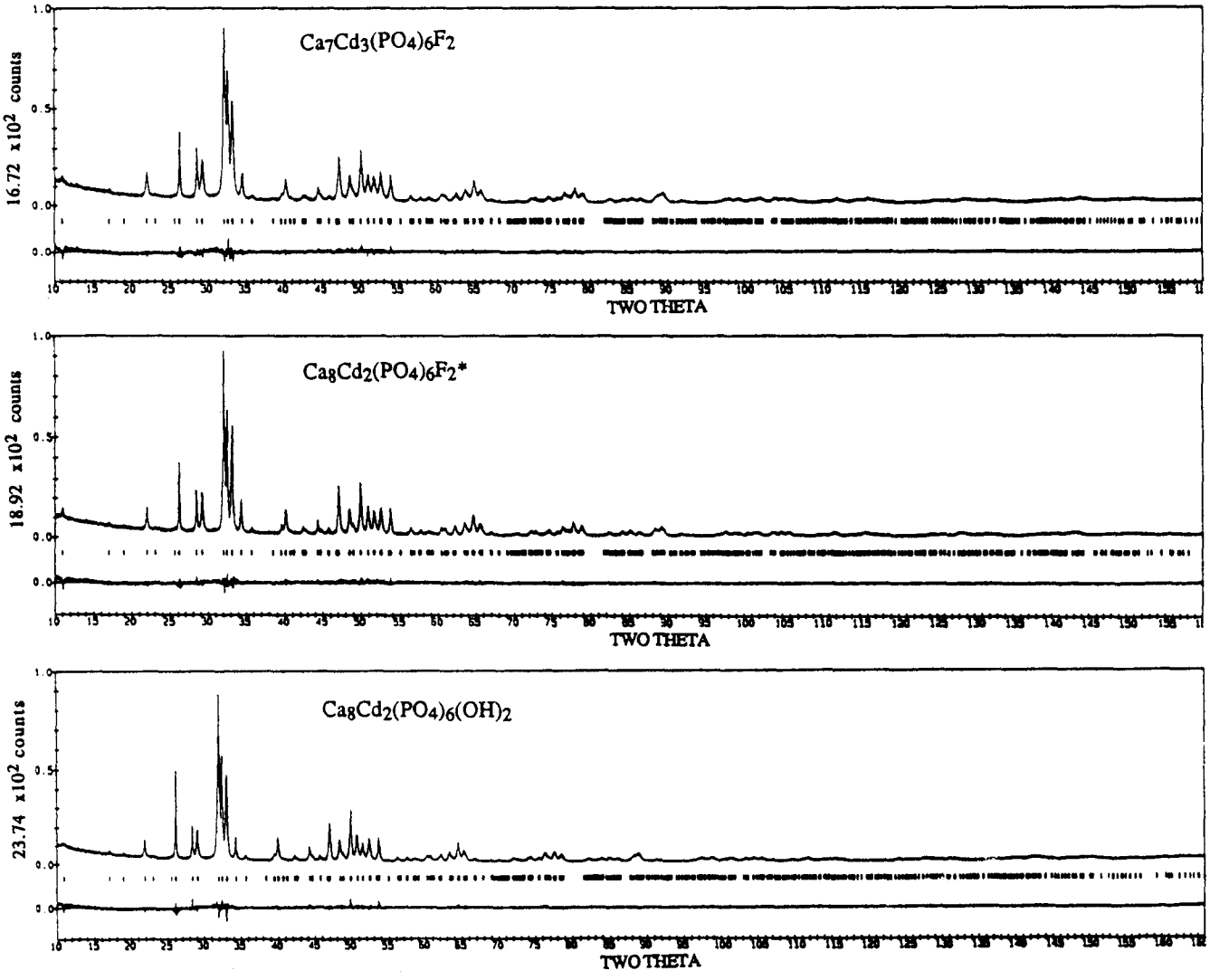

Fig. 2. The observed powder diffraction patterns. The lower pattern in each case is the difference between observed and calculated patterns.

(i) The nature of the anion placed in the channel is of great importance: in fluorapatite the Mn^{2+} ion (0.80 Å) substitutes for Ca I, and in chlorapatite the Mn^{2+} ion is randomly distributed at sites I and II [15].

(ii) The charge and the strength of the cation–anion bond is also important: for instance, in the case of rare earth substitution, whatever the radius of the ion a trivalent rare earth is located at site Ca II. This position is in agreement with the charge balance in a small area, and allows the formation of a strong rare earth–oxygen bond.

The Cd^{2+} radius (0.97 Å) is close to that of Ca^{2+} (0.99 Å). The results of structural refinement (Fig. 3) show that, whatever its amount in the apatite, cadmium is located simultaneously at the two cationic sites. Nevertheless, the distribution is not statistical. In fluorapatite, cadmium preferentially occupies site I and in hydroxyapatite site II.

We can notice that for fluorapatite this distribution is not in agreement with previous results of Piro *et al.* [16] who claimed that the cadmium distribution is dependent on the cadmium percentage in the apatite.

The difference for cadmium distribution between fluor- and hydroxyapatite is not correlated with the decrease in volume; indeed, the occupancies of the two sites are the same for each compound whatever the substitution percentage. These observed differences can certainly be attributed to the bond strength between cadmium and hydroxyl in hydroxyapatite and between cadmium and fluoride in fluorapatite.

Another point should be noted: whatever the preparation method (precipitation or solid–gas reaction), fluorapatite had the same cadmium distribution. So, in the case of the solid–gas reaction, which starts from an initial hydroxyapatite, one can assume that an intracrystalline migration of some of the cadmium from site II to site I occurs.

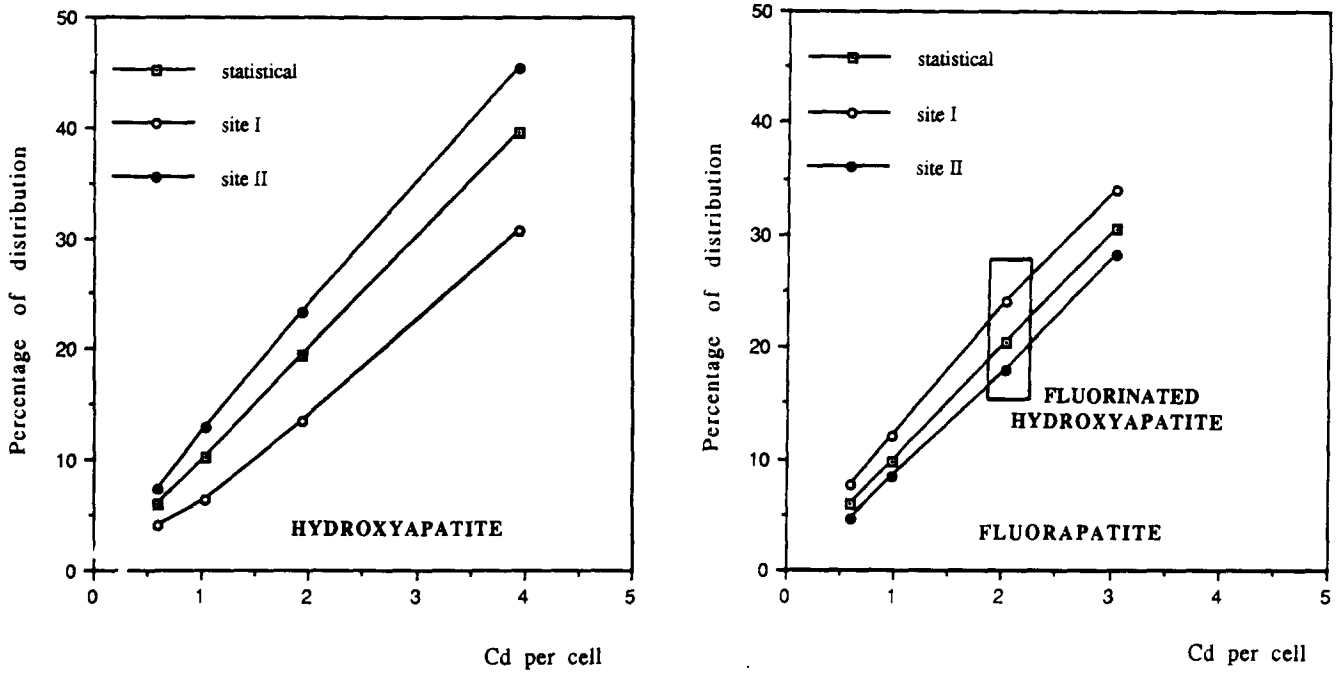

Fig. 3. Cadmium distribution in sites I and II.

Acknowledgment

We wish to thank the "Region Midi-Pyrenees" for financial support of this work.

References

1 R. Saint-Guilhem, *Proc. Int. Colloq. on Solid Phosphate Minerals, Toulouse, May 1967*, p. 9.
2 G. Montel, *Ann. Chim., 1* (1976) 177.
3 P.Fourman and P. Royer, *Calcium et Tissu Osseux — Biologie et Pathologie*, Flammarion, Paris, 1970, p. 23.
4 K. Sudarsanan and R. A. Young, *Acta Crystallogr. B, 25* (8) (1969) 1534.
5 R. A. Young, M. L. Bartlett, S. Spooner, P. E. Mackie and G. Bonel, *J. Biol. Phys., 9* (1981) 1.
6 D. McConnel, *Apatites*, Springer, New York, 1973.
7 R. Kreidler, *Ph.D. Thesis*, Pennsylvania University, 1967.
8 J. Brouwers and R. Lauwerys, *Arch. Mal. Prof. Med. Trav. Secur. Soc., 34* (3) (1973) 127.
9 Cadmium in phosphates: one part of wider environmental problem, *Phosphorus Potassium, 162* (July–August 1989) 23.
10 A. Nounah, J. Szilagyi and J. L. Lacout, *Ann. Chim. Fr., 15* (1990) 409.
11 H. M. Rietveld, *Acta Crystallogr., 22* (1967) 151.
12 R. A. Young and D. B. Wiles, *Adv. X-ray Anal., 24* (1981) 1.
13 D. B. Wiles and R. A. Young, *J. Appl. Crystallogr., 14* (1981) 149.
14 R. A. Young and D. B. Wiles, *J. Appl. Crystallogr., 15* (1982) 430.
15 J. L. Lacout, *Thèse*, Institut National Polytechnique de Toulouse, 1983.
16 O. E. Piro, M. C. Apella, E. J. Barran and B. E. Rivero, *Rev. Chim. Miner., 19* (1981) 11.